



Microstructure-related properties of explosively welded multi-layer Ti/Al composites after rolling and annealing

Monika Solecka¹ · Sebastian Mróz² · Paweł Petrzak¹ · Izabela Mania¹ · Piotr Szota² · Andrzej Stefanik² · Tomasz Garstka² · Henryk Paul¹

Received: 26 May 2022 / Revised: 25 October 2022 / Accepted: 19 November 2022 / Published online: 1 December 2022
© The Author(s) 2022

Abstract

The processes of rolling and annealing of explosively welded multi-layered plates significantly affect the functional properties of the composite. In current research, fifteen-layered composite plates were fabricated using a single-shot explosive welding technique. The composites were then rolled up to 72% to reduce layer thickness, followed by annealing at 625 °C for varying times up to 100 h. Microstructure evolution and chemical composition changes were investigated using scanning electron microscopy equipped with energy-dispersive spectroscopy. The mechanical properties of the composite were evaluated by tensile testing, while the strengths of individual layers near the interface were evaluated by micro-hardness measurements. After explosive welding, the wavy interfaces were always formed between the top layers of the composite and the wave parameters decreasing as the bottom layers approach. Due to the rolling process, the thickness of Ti and Al layers decreases, and the waviness of top interfaces disappeared. Simultaneously, the necking and fracture of some Ti layers were observed. During annealing, the thickness of layers with chemical composition corresponding to the Al₃Ti phase increased with annealing time. A study of growth kinetic shows that growth is controlled by chemical reaction and diffusion. The results of micro-hardness tests showed that after annealing, a fourfold increase of hardness can be observed in the reaction layers in relation to the Ti, while in relation to Al, the increase of hardness is even 15 times greater.

Keywords Multi-layer Al/Ti composite · Explosive welding · Hot-rolling · Annealing · Al₃Ti phase

1 Introduction

Parts in combat vehicles manufactured from homogeneous or multi-layer high-strength steel plates [1] are characterized by high specific gravity [2], which, in some cases can limit their applicability [3]. Therefore, research is being conducted at several research centers, looking into the possibility of using metallic materials that offer both high ballistic protection and the lowest possible specific gravity [4]. Since advanced armor usually consists of multiple layers of different materials that play a specific role in impact energy absorption, there are two ways to achieve the desired armor

properties [5]. One way is through the combined use of ceramics, plastics, and/or fiber-reinforced epoxy resins [6]. Another way is the construction of the layered composites based on high-strength light metals, like aluminum/steel [7], magnesium/aluminum/titanium [8] or aluminum/aluminum/titanium [9]. The latter solution proposed by Godzimirski et al. [10], Tasdemirci et al. [11] and Płonka et al. [12] includes composite-like multi-layer plates, mostly based on titanium (Ti) and aluminum (Al). Ti and Al and their alloys, as structural materials, attract attention due to their low density, high stiffness and strength-to-weight ratios, corrosion resistance, and high-temperature resistance (Ti) or good thermal conductivity (Al). Therefore, titanium–aluminum-based composites open up many new possibilities.

Welding of the Ti- and Al-based alloys is difficult due to the strong difference in melting points and very high reactivity concerning nitrogen and oxygen at high temperatures. Currently, there are many methods that can be used for the multi-layered Ti/Al composite fabrication through solid-state joining processes, e.g., using

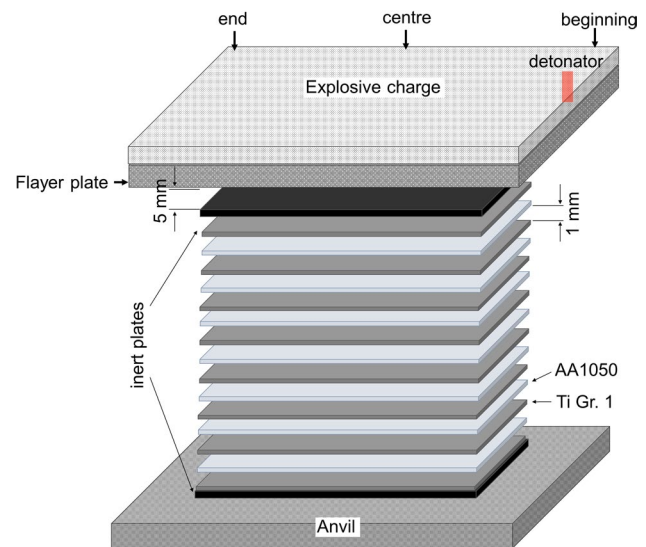
✉ Monika Solecka
m.solecka@imim.pl

¹ Institute of Metallurgy and Materials Science, Polish Academy of Sciences, Reymonta 25, 30-059 Kraków, Poland

² Faculty of Production Engineering and Materials Technology, Czestochowa University of Technology, J.H. Dąbrowskiego 69, 42-201 Częstochowa, Poland

Table 1 Chemical composition and mechanical properties of Ti and Al alloys used for the explosive welding process

Chemical composition (wt. %)												
Alloy	C	N	O	H	Cu	Mg	Si	Fe	Mn	Zn	Ti	Al
Ti Gr.1	0.08	0.03	0.18	0.015	-	-	-	0.2	-	-	Bal.	-
Al AA1050	-	-	-	-	0.05	0.05	0.25	0.4	0.05	0.07	0.05	Bal.
Mechanical properties												
Hardness (HBW)			Tensile Strength (MPa)				Yield Strength (MPa)			Modulus of Elasticity (GPa)		
Ti Gr.1	120		240				170				105	
Al AA1050	33		145				84				68	

**Fig. 1** Scheme for Ti(Gr. 1)/Al(AA1050) multi-layer EXW

accumulative roll-bonding (ARB) [13], hot-rolling [8], hot-pressing [14], or explosive welding (EXW) [15]. During ARB process, to reduce deformation resistance, it is necessary to isothermally heat-treat plates prior to the rolling. Thus, hot roll-bonding technology is a high-cost and overly complex process. Hot pressing seems to be a much more promising method in contrast to ARB process. However, this process enables to produce composites with limited size, determined by the size of the press machine. To produce a large-scale product, EXW method is successfully used. This method enables to join of a wide range of materials with different properties that are difficult or impossible to join by other methods. So far, several studies have described the various combinations of composites produced by EXW technique, such as Al/Cu proposed by Lokal et al. [16] and Paul et al. [17], Al/steel [18], Al/Mg proposed by Mroz et al. [19], Zeng et al. [20] and Paul [21], steel/Cu proposed by Dyja et al. [22], Andreevskikh [23] and Paul et al. [24], Al/Ti proposed by Bataev [25] and Paul [26], and many others.

Because no impurities are observed at the interfaces in multi-layer plates produced via explosive welding, migration of easy atoms to the adjacent layers occurs during post-welding heat treatment. (As shown by Bataev et al. [25], the dynamic of the diffusion in explosively welded composites is more than 3 times higher than in clads produced using the hot-pressing method). The structure modification via initiation of the diffusion processes leads to the formation of hard intermetallic layers. TiAl, Ti₃Al, and Al₃Ti phases are the most favorable intermetallic compounds in the Ti–Al binary systems. Zhang et al. [27] have shown that Al₃Ti phase has the lowest effective free energy, so it is easier to form at this interface. The Al₃Ti phase is of interest due to its light

weight, oxidation resistance at high temperatures, relatively high Young modulus (216 GPa), and low density (3.3 g/cm^3), which is lower than in Ti and Al-based compounds [28]. A strong increase in the performance of the composite can therefore be expected by introducing hard intermetallic layers based on the Al_3Ti phase into the structure.

The aim of the current research is to investigate the phenomena that occur at the interfaces of fifteen-layered Al/Ti composite. Special attention was paid to the dynamic of the intermetallic phase growth leading to the disappearance of the soft (Al) components. Single-shot EXW process was used to produce multi-layered composite, whereas hot-rolling was applied to reduce the thickness of individual layers. Finally, the heat treatment at $625 \text{ }^\circ\text{C}$ for times ranging between 1 and 100 h was applied to induce intermetallic phase growth. Subsequently, analysis of the growth dynamic was performed to determine the factors controlling the quality of interfacial layers. The analyses were conducted using scanning electron microscopy (SEM) equipped with back-scattered electron (BSE) and X-ray energy-dispersive spectrometry (EDS) detectors. The microstructural analyses were correlated with micro-hardness measurements.

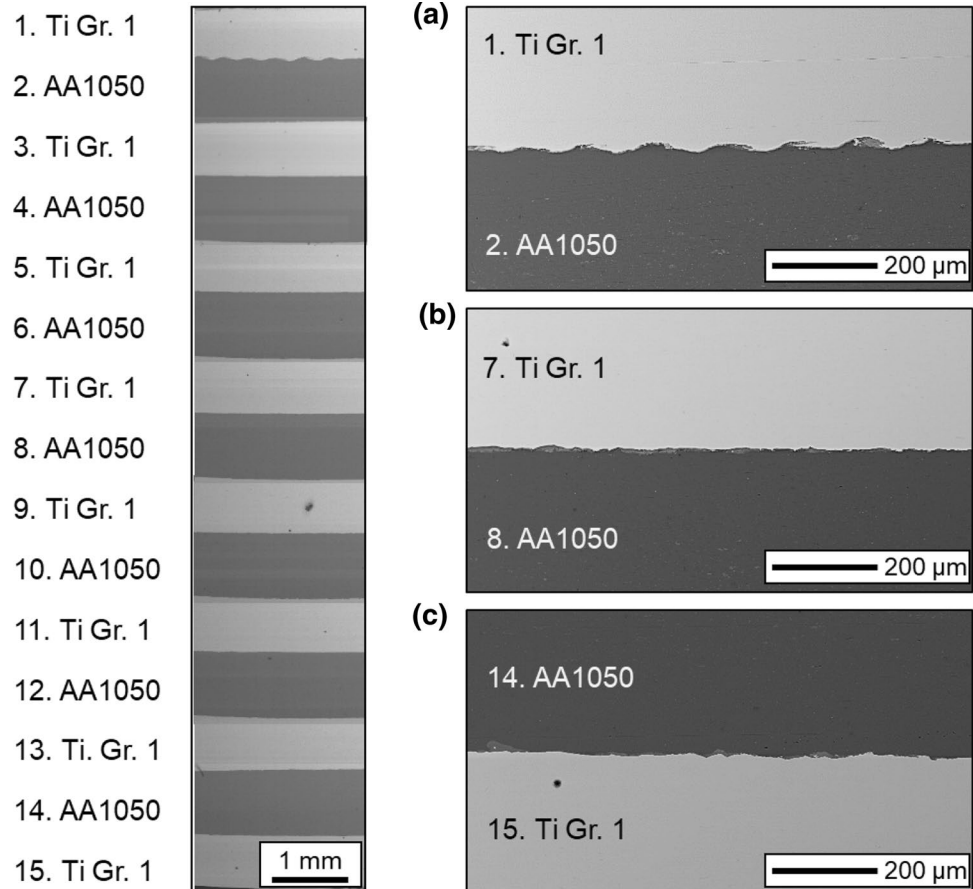
2 Materials and methods

2.1 Materials and explosive welding

The tested plate was composed of eight sheets of Ti Gr. 1 (hereafter denoted as Ti) and seven sheets of AA1050 alloy (hereafter denoted as Al). The sheets' size was $210 \text{ (length)} \times 300 \text{ (width)} \text{ mm}^2$. The materials of the sheets in the initial state were characterized by a uniform, fully recrystallized microstructure. The chemical composition and mechanical properties of Ti and Al alloys are given in Table 1. The thickness of the Ti and Al sheets was 1 mm.

EXW was conducted by High Energy Techniques Works 'Explomet' (Opole, Poland). The single-shot explosion welding technique was applied to form a fifteen-layered plate composed of alternatively arranged Ti and Al sheets. In the applied set-up, the top and bottom layers were always Ti. The composites were obtained using the constant stand-off explosive cladding technique with an initial 1 mm stand-off distance between the layers, 5 mm thick flyer sheet, and steel anvil. Before welding, the contact surfaces of the joined sheets were ground, cleaned of solid contaminants, and degreased. A detonator was placed in the middle of the

Fig. 2 Cross section of 15-layer Ti/Al composite after EXW showing an overview of the sample cross section and details of **a** 1st, **b** 7th, and **c** 14th interface



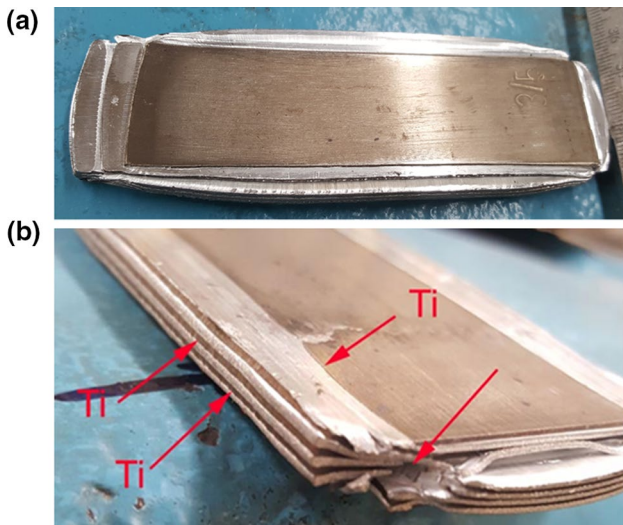


Fig. 3 View of the samples after the first pass (a) and after the second pass (b)

Table 2 Sample height and applied reduction of the composite during hot-rolling

Pass no	sample height [mm]	height reduction per pass [%]	total height reduction [%]
0	12.8		
1	7.0	45	45
2	3.6	49	72

shorter edge of the flyer plate. A modified Saletrol explosive charge with a layer thickness of 30 mm was used to initiate a detonation velocity of 2320 m/s. An Explomet-Fo-2000

measuring instrument (Kontinitro) was used to measure the detonation velocity. It is an electronic timer for which light signals initiate and stop measuring. The scheme for Ti/Al multi-layer single-shot EXW is presented in Fig. 1.

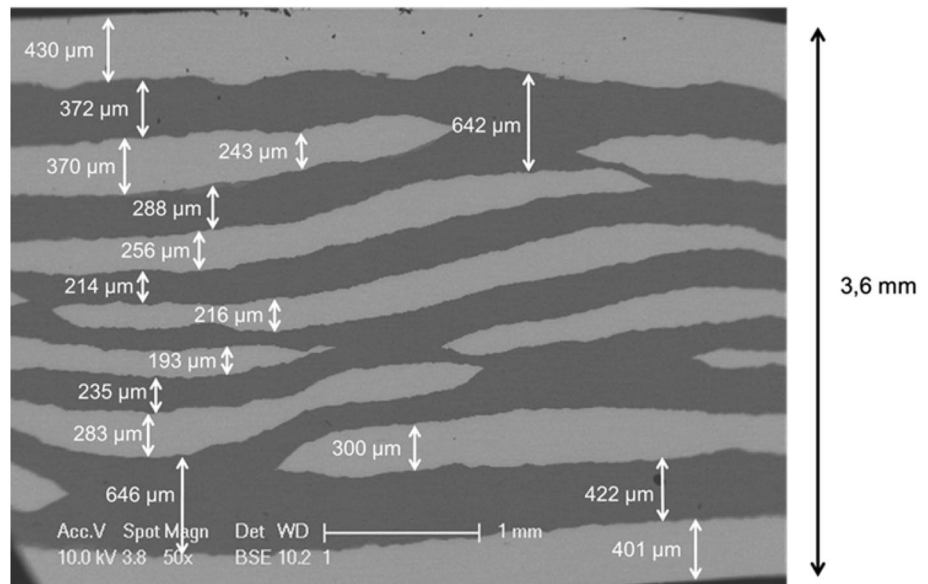
2.2 Hot-rolling and annealing processes

The EXW plates were then hot-rolled using a semi-industrial rolling mill (D300 mm). The thermoplastic processing was performed in two passes at 430 °C up to a total thickness reduction of 72%. The rolling speed was 0.2 m/s. For the rolling process, the specimen with dimensions of 13 × 30 × 100 mm³ was cut from the EXW plate. The samples were prepared in a way that the rolling direction (RD) was parallel to the detonation direction (DD). Materials before rolling were annealed in a laboratory furnace at 450 °C for 20 min, then the annealed material was quickly transferred to the rolling mill. The time between transferring material from the furnace to the rolling mill was less than 5 s. The multi-layer feedstock was heated in the LAC KC 120/14 resistance chamber furnace before the individual passes. After the rolling process, the samples with dimensions of 15 × 5 × 2 mm³ were cut off from the middle section of the rolled sheets. Then the samples were annealed at 625 °C for times ranging between 1 and 100 h using a furnace without a protective atmosphere.

2.3 Microstructure observation, tensile test and micro-hardness measurements

The samples for microscopic observations were cut along the DD from EXW plates and along RD from

Fig. 4 SEM/BSE image showing Ti/Al composite after hot-rolling



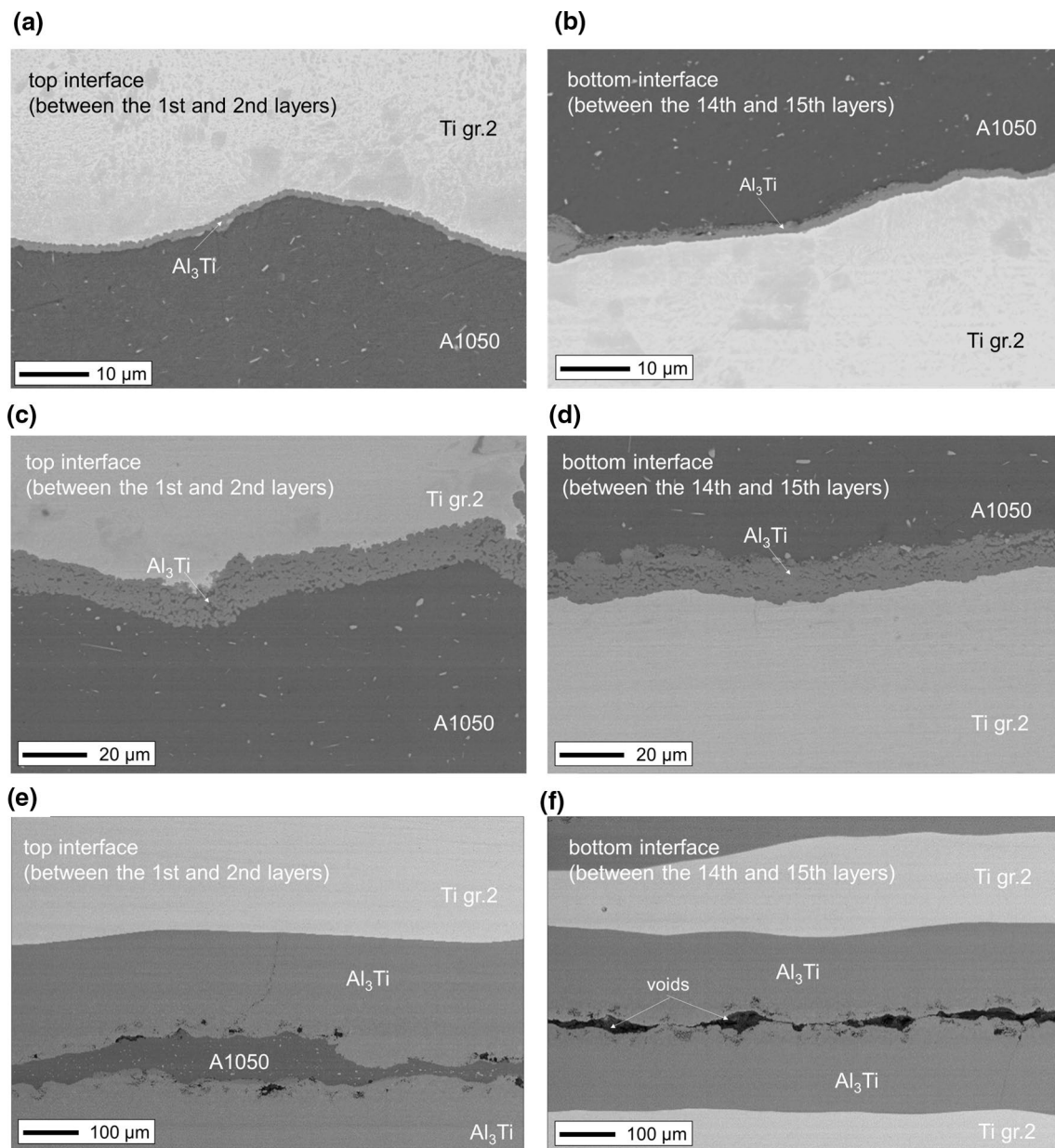


Fig. 5 SEM/BSE images showing the growth of reaction layer after hot-rolling and annealing at 625 °C for 1 h (a, b), 10 h (c, d), and 100 h (e, f)

post-annealed hot-rolled sheets, using a wire saw. The metallographic examinations of samples were carried out using an optical microscope (OM) and SEM (XL30 Philips) equipped with a BSE and EDS detectors. The tensile tests were carried out at room temperature (RT) using an Instron Model 6065 Universal Testing Machine with a strain rate of 0.00025 s^{-1} . The tensile samples were cut perpendicular to the rolling direction of the composite sheets. Dog-bone-shaped tensile specimen with a thickness 5 mm, a width of the test section of 3 mm, and the length of 40 mm was machined with the use of electrical discharge saw. Three tensile specimens were tested for each

type of materials (3 specimens after hot-rolling as well as 3 specimens after hot-rolling and annealing at 625 °C for 100 h). The ultimate tensile strength, yield strength, and elongation were determined from the stress–strain curves.

Vickers micro-hardness measurements were conducted on finely polished surfaces on ND/(DD or RD) sections to identify the micro-hardness of the reaction regions near the joint surface. The measurements were performed with a load of 100 G ($HV_{0.1}$) and a dwell time of 15 s. The obtained micro-hardness values were given as the average of three indentation measurements.

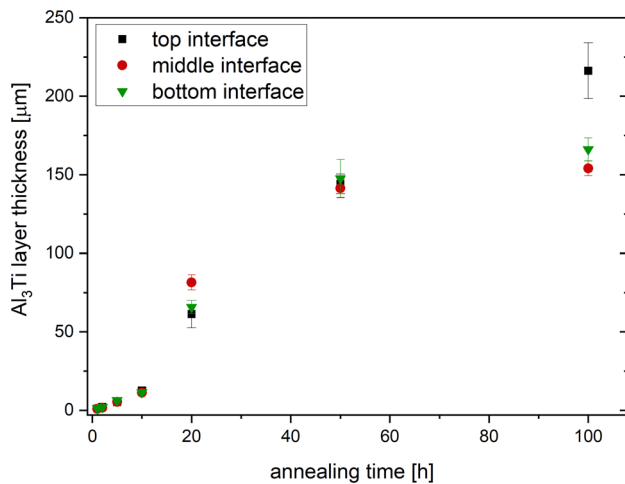


Fig. 6 Changes in the average thickness of the reaction layer at the top, middle, and bottom interfaces after annealing

3 Results and discussion

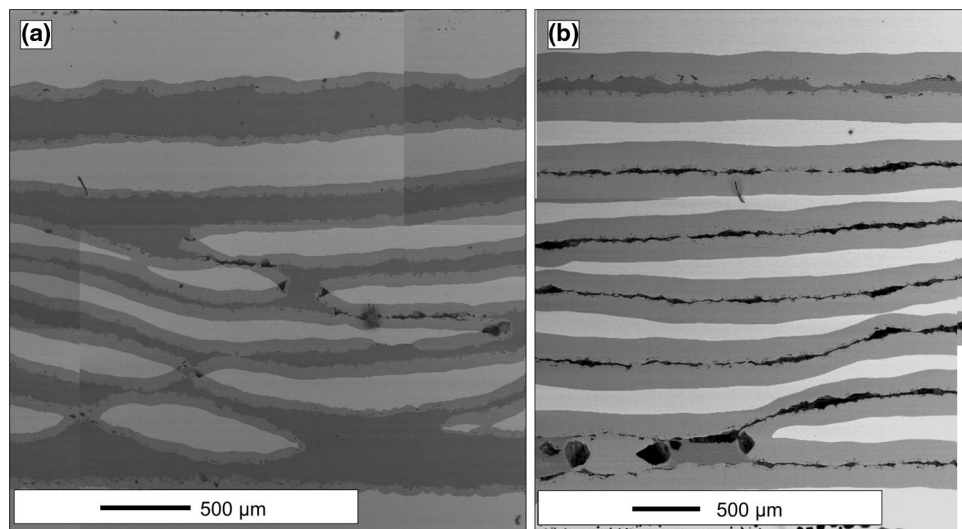
3.1 Macroscopic observations

Figure 2 shows the structure of the composite, in the as-welded state, typically observed in the ND/DD section. Strong variation of the interface morphology was observed across the clad thickness. The formation of the wavy interface between the first two (top) layers of the composite located near the flyer plate, i.e., close to the explosive charge, is well visualized (Fig. 2a). In contrast, the interfaces between the layers in the middle and at the bottom of the composite were almost flat (Figs. 2b, c). The changes in the morphology of the contacting layers were due to the formation of wave-type features reflecting turbulent

flow of layers near the interface. The beginning of the first interface had the strongest waviness, whereas the interfaces between plates at the bottom part of the composite were nearly flat. The result of this observation corresponds to earlier studies by Bataev et al. [25], Paul et al. [26], and Petrzak et al. [29], who showed that clads produced by EXW perform significantly different in the interface morphology across the composite thickness and along its length. They also observed that the wave amplitude linearly depends on the kinetic energy loss due to the collision of the sheets. This energy rapidly decreases with each successive collision of the sheets. Morphological changes are also due to the occurrence of melted regions. In the upper layers, these reaction regions are mainly located in the wave vortices and on the wave crests. In the middle and bottom parts of the composite, they take a form of (semi)continuous layers situated along the interfaces. However, a decreasing quantity of the reaction regions can be observed as the bottom surface of the composite is approached.

Figure 3 shows the structure of the EXW plate after a two-pass hot-rolling. After this process, the total thickness of the plate was reduced by 72% (Table 2) up to 3.6 mm. The thicknesses of individual layers were reduced up to 190–430 μm and 210–420 μm for Al and Ti, respectively, whereas the wave amplitude of the upper layers decreased significantly. Simultaneously, the discontinuities of the Ti layers were observed (Fig. 4). In the study of Assari and Eghbali [30], such discontinuities are associated with necking and subsequent crack formation of Ti layers; these phenomena are thought to be caused by the lower ductility of Ti as compared to Al. In the areas, where discontinuities of Ti layers occur, Al layers merge. This locally increases the thickness of Al layers up to 600–650 μm. Since the specimen with an initial width-to-height ratio of 2.4 was used in

Fig. 7 SEM/BSE images showing discontinuities formation after hot-rolling and annealing at 625 °C for: **a** 20 h and **b** 100 h



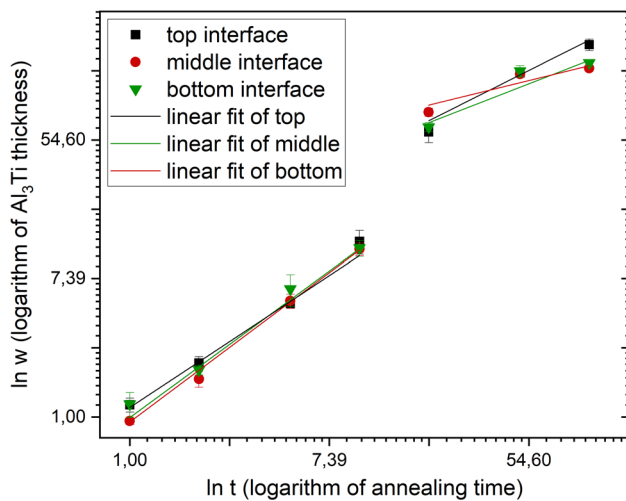


Fig. 8 The plot of $\ln w$ versus $\ln t$ by linear fit analysis

the rolling process, an intense plastic flow of the individual layers in both the RD and TD sections was observed. This was especially well observed for the Al layers, which were extruded intensively from between the Ti layers (Fig. 3).

4 The dynamic of the Al_3Ti phase growth

The kinetic of the intermetallic phase growth during heat treatment of EXW and/or hot-rolled composites has been the subject of many studies, e.g., Lazurenko et al. [15], Petrzak

et al. [29] and Fronczek et al. [31]. Most of them were conducted at temperature ranges between 550 and 640 °C. The results of these tests vary, depending on the thickness of the sheets and bonding parameters, such as detonation velocity or stand-off distance, between layers applied during the process.

Figure 5 shows the SEM/BSE microstructure of hot-rolled Ti/Al sheets after heat treatment at 625 °C and for annealing times ranging between 1 and 100 h, while changes of the intermetallic layer thickness as a function of time are shown in Fig. 6. After the annealing time of 1 h, the thickness of the intermetallic layers reached ~1.9 μm and ~1.2 μm for the top (Fig. 5a) and bottom (Fig. 5b) interfaces respectively, whereas in the center of the composite, it is significantly smaller (~0.9 μm). Extending the annealing time up to 2 h caused double increase in the thickness of the intermetallic layers, in all three areas tested. Uniformity of the thickness of the intermetallic layer across the composite thickness was observed in the range of annealing times up to 10 h (Fig. 5c, d), with an increase of the intermetallic phase up to 12 μm observed. Increase of annealing time to 100 h (Fig. 5e, f), contributes to significant increase of the width of the intermetallic layers. However, areas where the Al layers were not completely consumed were observed. This can be seen in Fig. 7b, which shows unreacted areas at the top and bottom layers of the composite, while the middle layers of Al are fully reacted. Comparing the microstructures in Figs. 4 and 7a, differences in the width of the Al layers in the different parts of the composite are observed; the Al layers in the

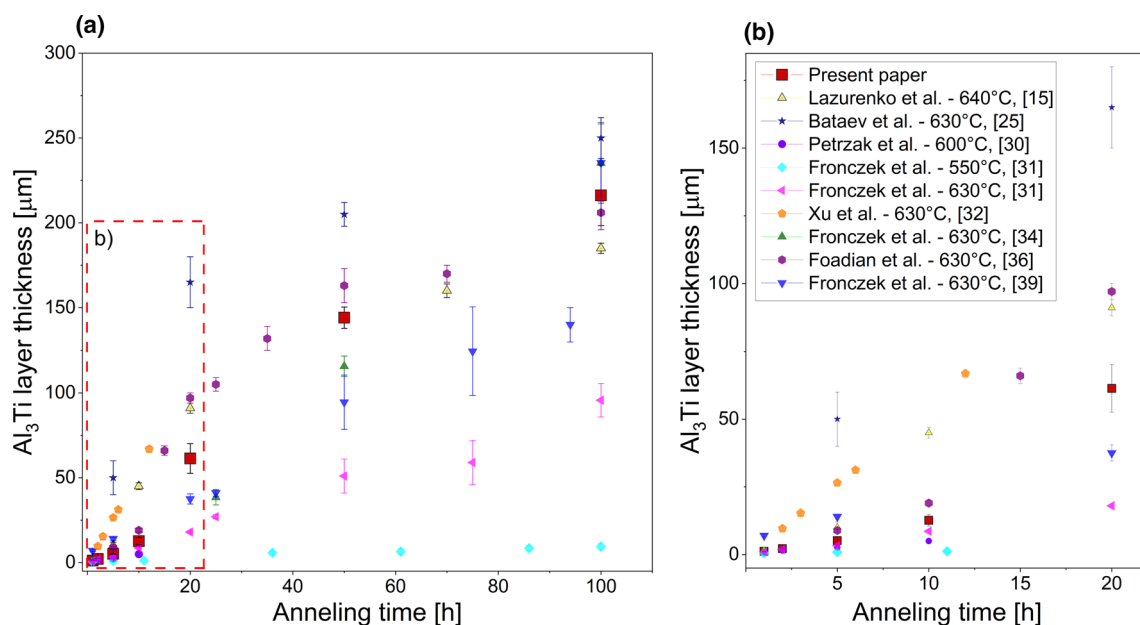


Fig. 9 Total width of the reaction layer formed upon annealing at 625 °C for between 1 h and 100 h. The results are compared with those obtained by: Lazurenko et al. [15]; Bataev et al. [25]; Petrzak et al. [30]; Fronczek et al. [31, 34, 39]; Xu et al. [32] and Foadian et al. [36]

Table 3 Summary of current research on mechanism controlling reaction layer growth compared to the literature studies

Present paper	Petrzak et al. [2019]	Fronczek et al. [2018]	Fronczek et al. [2017]	Fronczek et al. [2016]	Fronczek et al. [2016]	Lazurenko et al. [2016]	Foadian et al. [2014]	Bataev et al. [2012]	Xu et al. [2006]
The temperature of annealing [°C]	600	630	630	550	630	640	630	630	630
Number of inter-faces	14	2	2	1	1	39	5	20	9
Detonation velocity [m/s]	2600	1900±50	1900±50	1900±50	1900±50	4200	4500	4200	Not specified
Annealing conditions	Air, hot-pressing	Vacuum	Vacuum	Vacuum	Vacuum	Air	Ambient	Air	Vacuum
Mechanism of Al ₃ Ti phase growth	NS	SCR, VD and CR	VD and CR	VD	CR	SD	DF and CR	NS	DF

DF diffusion, SD solely diffusion, VD volume diffusion, CR chemical reaction, SCR solely chemical reaction, NS not specified

Table 4 Mechanical properties of the platers after hot-rolling and after hot-rolling and annealing at 625 °C for 100 h

Configuration	Rm [MPa]	R0.2 [%]	A [%]
Hot-rolling	331.21	303.16	20.4
Hot-rolling + annealing	105.55	94.06	13.0

upper and lower regions are much wider than in the middle region of the sample, Fig. 7a.

The SEM/EDS chemical composition measurements revealed the presence of layers consisting of 71% of Al and 29% of Ti, suggesting a formation of the Al₃Ti intermetallic phase. It was the only intermetallic compound formed independently during the applied annealing time. This result is consistent with previous work by Xu et al. [32] and van Loo and Rieck [33], who reported that Al₃Ti is the only phase that can be observed at the Ti/Al interface (Gibbs free energy for the formation of the Al₃Ti phase was substantially lower than those of other stable phases). Similar results on multi-layered composites were reported by Lazurenko et al. [15], Petrzak et al. [29] and Fronczek et al. [34], who documented that the heat treatment of Al/Ti composite led to the rapid growth of layers composed of the Al₃Ti intermetallic phase along the entire interface. It has also been documented in these works that the areas of primary melted regions composed of several non-equilibrium phases, i.e., not observed on Al–Ti equilibrium phase diagram, are transformed during heat treatment (via atoms migration) into the equilibrium Al₃Ti phase. Since the solubility of Al in Ti is 3 times greater than the solubility of Ti in Al, therefore Al layers are consumed significantly faster than Ti ones. Annealing time strongly influences the rate of the Al₃Ti phase growth. Dybkov [35] and Foadian et al. [36] described the growth of the Al₃Ti phase as a process controlled by two different mechanisms—diffusion and/or chemical reaction. The growth of the reaction layer during annealing can be expressed via the well-known equation $w = kt^n$ [37], which relates the width of the reaction layer (w) to the annealing time (t). The parameters k and n are constants. It is widely accepted that the value of n determines the mechanism responsible for the growth of the reaction layer; if n is close to 1, the growth process is controlled by chemical reactions, while if it is close to 0.5, the growth process is controlled by diffusion. The plot of $\ln(w)$ versus $\ln(t)$ is shown in Fig. 8.

In the range of annealing times analyzed, strong changes in the n value are observed. For annealing times up to 10 h, the value of n is close to 1, which suggests that growth of the Al₃Ti layer is controlled by a chemical reaction. This is mainly due to the small distance between the Al and Ti layers, which facilitates faster mutual diffusion across the interfaces. For annealing times above 20 h, the n value is close to 0.5, suggesting that the growth of the Al₃Ti layer is mainly

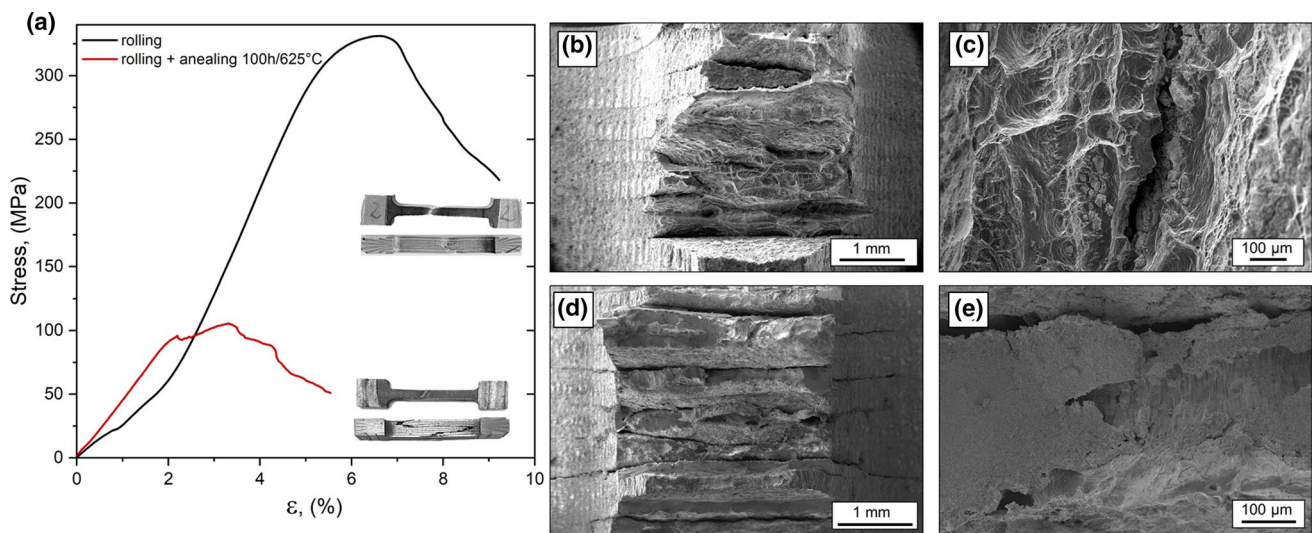


Fig. 10 Representative stress–strain curves obtained for samples after hot-rolling and after hot-rolling and annealing (a) as well as SEM/SE images showing fracture morphology of the sample after hot-rolling (b, c) and after hot-rolling and annealing at 625 °C for 100 h (d, e)

controlled by diffusion. The chemical reaction is hindered because it occurs through the already formed Al_3Ti layer.

The growth kinetics of the Al_3Ti phase in explosively welded composites has been the subject of many studies. Foadian et al. [38], Bataev et al. [25], Fronczek et al. [31, 34, 39] and Xu et al. [32] analyzed this aspect during the annealing at 630 °C. Studies of growth kinetics at 640 °C were carried out by Lazurenko et al. [15], whereas at 600 and 550 °C by Petrzak et al. [29] and by Fronczek et al. [31], respectively. Figure 9 and Table 3 present a change in values of the average thickness of the reaction layer measured in the current research and a comparison with previously obtained literature data. It can be concluded that different mechanisms are responsible for the growth of the reaction layers. It may be related with different parameters applied during bonding which results in strongly different microstructural changes near the interface. However, in majority of the analyses, the kinetic of growth occurred as result of volume diffusion or chemical reaction (Table 3). Study on growth of the reaction layer carried out at 550 °C by Fronczek et al. [31] showed that bulk diffusion was dominant. However, Thiyaneshwaran et al. [40] showed that, in addition to the diffusion mechanism, chemical reaction also plays a significant role.

To evaluate the mechanical properties of the clad and in particular intermetallic phase, the tensile stress and micro-hardness measurements were carried out.

Results of the tensile test for the hot-rolled and post-annealed hot-rolled composite (annealing at 625 °C for 100 h) are summarized in Table 4, and representative stress–strain curves are shown in Fig. 10a. The general conclusion is that the hot-rolled composites show higher mechanical properties compared to the hot-rolled and

annealed composites—maximum tensile strength (R_m) for the hot-rolled composite was 331.2 MPa, whereas for the hot-rolled and annealed composite was 105.6 MPa. Similarly, the yield strength values ($R_{0.2}$) were 303.2 and 94.1 MPa, for the hot-rolled and post-annealed hot-rolled composite, respectively. The relative elongation (A_5) for hot-rolled composites was 20.4%, while for annealed hot-rolled ones, it was 13.0%.

Tensile tests for hot-rolled state revealed ductile character of fracture—(Fig. 10b, c), crack and numerous cavities are visible (Fig. 10c), forming a typical cup-and-cone surface. In contrast, brittle fractures were observed in the composites after hot-rolling and annealing at 625 °C for 100 h (Fig. 10d, e). Numerous delaminations were also observed in the interface areas between the Ti and Al_3Ti phases.

Micro-hardness measurements were performed on the longitudinal section across the interface and the results are shown in Fig. 11. In the ‘as-welded’ state, large micro-hardness gradients close to the interfaces, resulting from a strong strengthening of the jointed sheets, can be observed. The micro-hardness results range between 37 and 43 $\text{HV}_{0.1}$ for Al and 186 to 213 $\text{HV}_{0.1}$ for Ti. In the case of Al, the increased micro-hardness is limited to a thin layer close to the joint surface, while Ti undergoes strong strengthening over a much longer distance. The results of micro-hardness measurements for sample after 1 h annealing (Fig. 10b) showed a slight decrease in the hardness of the jointed materials. The hardness values vary from 29 to 33 $\text{HV}_{0.1}$ and from 158 to 181 $\text{HV}_{0.1}$ for Al and Ti, respectively. On the other hand, significant increase of micro-hardness after longer annealing times is related to the presence of the intermetallic layers. After annealing for 100 h (Fig. 10d), micro-hardness

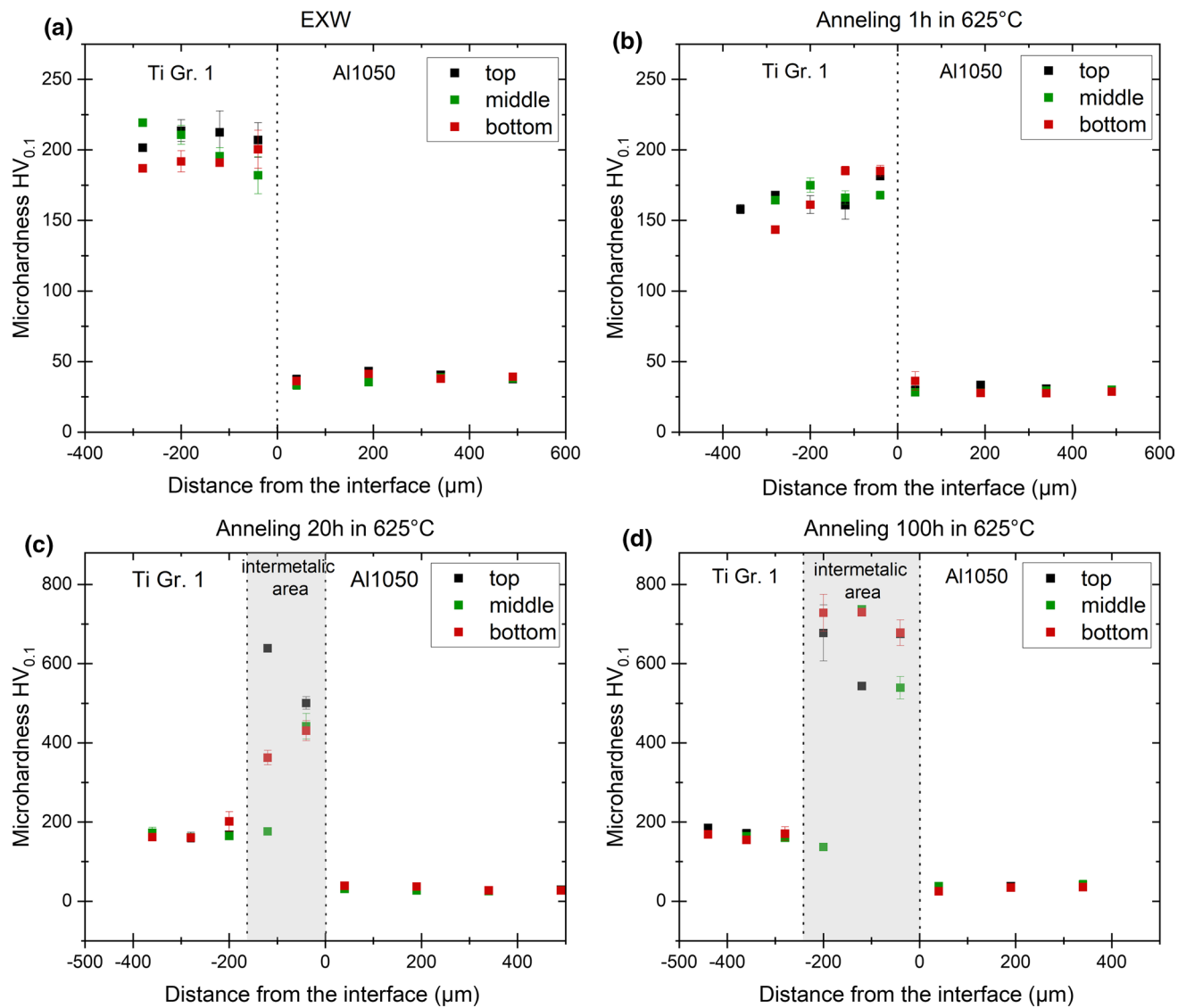


Fig. 11 Variation in the micro-hardness on the ND/DD sections after **a** EXW, rolling and annealing at 625 °C for **b** 1 h, **c** 20 h and **d** 100 h

measured in Al and Ti are $\sim 180 HV_{0.1}$ and $\sim 34 HV_{0.1}$, respectively. Reaction region is characterized by microhardness values ranged between $550 HV_{0.1}$ and $677 HV_{0.1}$. According to Hu et al. [41], the Al_3Ti phase possesses high hardness, which is related to high shear modulus and low bulk modulus. Nevertheless, these parameters may have an impact on voids formation, especially between two intermetallic faces to $Ti/Al_3Ti-Al_3Ti/Ti$ (Fig. 5f and Fig. 7b).

5 Conclusion

The kinetics of the intermetallic phase growth in Al/Ti-based composites fabricated using explosive welding technology subjected to hot-rolling and annealing processes were

analyzed in this study. A 72% thickness reduction of the fifteen-layered Ti/Al composite was achieved by hot-rolling in two passes. During subsequent heat treatment at 625 °C, the Al layers reacted with Ti, forming a reaction layer with a chemical composition corresponding to the Al_3Ti phase. SEM/BSE analyses of hot-rolled and then annealed samples for times ranging between 1 and 100 h showed the systematic growth of a continuous layer of the intermetallic phase along all the interfaces, leading to the formation of a $Ti/Al_3Ti/\dots/Al_3Ti/Ti$ -type composite. It was documented that due to the annealing process carried out for 100 h, almost all Al layers reacted. However, insignificant amount of unreacted Al was still observed. The growth of the reaction layer is governed by a chemical reaction in the first stage and controlled diffusion in the second stage. This resulted

in linear growth kinetics in the first stage and parabolic in the second stage.

The results of micro-hardness tests showed that long-term heat treatment results in a fourfold increase of hardness within the reaction layers with respect to the Ti layer, while as compared to the Al, the hardness value is even 15 times greater. However, the tensile tests revealed a formation of delamination between the Ti/Al₃Ti interfaces which decrease mechanical properties of Ti/Al composite after annealing at 625 °C for 100 h.

Acknowledgements The authors give special thanks to Mr. A. Gałka from 'Explomet' (Opole, Poland) for supplying the fifteen-layered Ti/Al composites.

Funding The authors gratefully acknowledge the financial support of the National Science Centre (Poland) under grant no. 2016/21/B/ST8/00462 and by the National Center for Research and Development (NCBiR), Poland, grant no. TECHMATSTRATEG2/412341/8/NCBR/2019 (EMuLiReMat).

Data availability Data can be supplied upon request.

Declarations

Conflict of interest The authors declare that they have no known competing financial interests or personal relationships that could have appeared to influence the work reported in this paper.

Ethical approval This article does not contain any studies with human participants or animals performed by any of the authors.

Open Access This article is licensed under a Creative Commons Attribution 4.0 International License, which permits use, sharing, adaptation, distribution and reproduction in any medium or format, as long as you give appropriate credit to the original author(s) and the source, provide a link to the Creative Commons licence, and indicate if changes were made. The images or other third party material in this article are included in the article's Creative Commons licence, unless indicated otherwise in a credit line to the material. If material is not included in the article's Creative Commons licence and your intended use is not permitted by statutory regulation or exceeds the permitted use, you will need to obtain permission directly from the copyright holder. To view a copy of this licence, visit <http://creativecommons.org/licenses/by/4.0/>.

References

- Wiśniewski A. Pancerze-budowa, projektowanie i badania. Warszawa: WNT; 2001. ((in polish)).
- Gooch W, Burkins M, Squillaciotti R, Koch RMS, Oscarsson H, Nash C. Ballistic testing of Swedish steel ARMOX Plate for US armor applications 21st Int Symp Ballist, Adelaide. South Australia. 2004;19:23.
- Børvik T, Dey S, Clausen AH. Perforation resistance of five different high-strength steel plates subjected to small-arms projectiles. *Int J Impact Eng*. 2009. <https://doi.org/10.1016/j.ijimpeng.2008.12.003>.
- Boccaccini AR, Atiq S, Boccaccini DN, Dlouhy I, Kaya C. Fracture behaviour of mullite fibre reinforced-mullite matrix

- composites under quasi-static and ballistic impact loading. *Compos Sci Technol*. 2005. <https://doi.org/10.1016/j.compscitech.2004.08.002>.
- Odanović Z, Bobić B. 2003 Ballistic protection efficiency of composite ceramics/metal armours. *Sci. Rev*. <http://www.vti.mod.gov.rs/ntp/rad2003/3-03/odan/odan.pdf>.
- Cheeseman BA, Bogetti TA. Ballistic impact into fabric and compliant composite laminates. *Compos Struct*. 2003. [https://doi.org/10.1016/S0263-8223\(03\)00029-1](https://doi.org/10.1016/S0263-8223(03)00029-1).
- Pedersen KO, Børvik T, Hopperstad OS. Fracture mechanisms of aluminium alloy AA7075-T651 under various loading conditions. *Mater Des*. 2011. <https://doi.org/10.1016/j.matdes.2010.06.029>.
- Wachowski M, Kosturek R, Śniezek L, Mróz S, Stefanik A, Szota P. The effect of post-weld hot-rolling on the properties of explosively welded Mg/Al/Ti multilayer composite. *Materials (Basel)*. 2020. <https://doi.org/10.3390/MA13081930>.
- Boroński D, Kotyk M, Maćkowiak P, Śniezek L. Mechanical properties of explosively welded AA2519-AA1050-Ti6Al4V layered material at ambient and cryogenic conditions. *Mater Des*. 2017. <https://doi.org/10.1016/j.matdes.2017.08.008>.
- Godzimirski J, Janiszewski J, Rośkowicz M, Surma Z. Ballistic resistance tests of multi-layer protective panels. *Eksploata i Niezawodn*. 2015;17:416.
- Tasdemirci A, Hall IW. Development of novel multilayer materials for impact applications: A combined numerical and experimental approach. *Mater Des*. 2009. <https://doi.org/10.1016/j.matdes.2008.07.054>.
- Płonka B, Remsak K, Rajda M. Badania. 2018 balistyczne demonstratorów opancerzenia dodatkowego. *Szybkobieżne Pojazdy Gąsienicowe*. (in polish).
- Li Y, Liu C, Yu H, Zhao F, Wu Z. Numerical simulation of Ti/Al bimetal composite fabricated by explosive welding. *Metals (Basel)*. 2017. <https://doi.org/10.3390/met7100407>.
- Kowalski W, Paul H, Petrzak P, Maj Ł, Mania I, Faryna M. Influence of hot pressing on the microstructure of multi-layered Ti/Al composites. *Mater: Arch. Metall*; 2021. p. 66.
- Lazurenko DV, Bataev IA, Mali VI, Bataev AA, Maliutina IN, Lozhkin VS, Esikov MA, Jorge AMJ. Explosively welded multi-layer Ti-Al composites: Structure and transformation during heat treatment. *Mater Des*. 2016. <https://doi.org/10.1016/j.matdes.2016.04.037>.
- Lokaj J, Sahul M, Sahul M, Nesvadba P. 2019 Investigation of properties of Cu-Al explosively welded bimetal. *High Energy Mater*. <https://doi.org/10.2221/1matwys/0179>
- Paul H, Lityńska-Dobrzyńska L, Prażmowski M. Microstructure and phase constitution near the interface of explosively welded aluminum/copper plates. *Metall: Mater. Trans. A Phys. Metall. Mater. Sci*; 2013. <https://doi.org/10.1007/s11661-013-1703-1>.
- Chen X, Inao D, Tanaka S, Mori A, Li X, Hokamoto K. Explosive welding of Al alloys and high strength duplex stainless steel by controlling energetic conditions. *J Manuf Process*. 2020. <https://doi.org/10.1016/j.jmapro.2020.09.037>.
- Mroz S, Stradomski G, Dyja H, Galka A. Using the explosive cladding method for production of Mg-Al bimetallic bars. *Arch Civ Mech Eng*. 2015. <https://doi.org/10.1016/j.acme.2014.12.003>.
- Zeng X, Wang Y, Li X, Li X, Zhao T. Effect of inert gas-shielding on the interface and mechanical properties of Mg/Al explosive welding composite plate. *J Manuf Process*. 2019. <https://doi.org/10.1016/j.jmapro.2019.07.007>.
- Paul H, Petrzak P, Chulist R, Maj Ł, Mania I, Prażmowski M. Effect of impact loading and heat treatment on microstructure and properties of multi-layered AZ31/AA1050 plates fabricated by single-shot explosive welding. *Mater Des*. 2022. <https://doi.org/10.1016/j.matdes.2022.110411>.

22. Dyja H, Mroz S, Stradomski Z. Properties of joint in the bimetallic rods Cu-Al and Cu-steel after explosive cladding and the process of rolling. *Metalurgija*. 2003;42:185–91.
23. Andreevskikh LA, Drozdov AA, Mikhailov AL, Samarokov YM, Skachkov OA, Deribas AA. Producing bimetallic steel-copper composites by explosive welding. *Steel Transl*. 2015. <https://doi.org/10.3103/S0967091215010027>.
24. Paul H, Chulist R, Lityńska-Dobrzyńska L, Prazmowski M, Faryna M, Mania I, Szulc Z, Miszczyk MM, Kurek A. Interfacial reactions and microstructure related properties of explosively welded tantalum and steel sheets with copper interlayer. *Mater Des*. 2021. <https://doi.org/10.1016/j.matdes.2021.109873>.
25. Bataev IA, Bataev AA, Mali VI, Pavliukova DV. Structural and mechanical properties of metallic-intermetallic laminate composites produced by explosive welding and annealing. *Mater Des*. 2012. <https://doi.org/10.1016/j.matdes.2011.09.030>.
26. Paul H, Maj Ł, Prazmowski M, Gałka A, Miszczyk M, Petrzak P. Microstructure and mechanical properties of multi-layered Al/Ti composites produced by explosive welding. *Procedia Manuf*. 2018. <https://doi.org/10.1016/j.promfg.2018.07.343>.
27. Zhang H, Zhang N, Jia Q, Li D. Calculation and experimentation on the formation sequence of compounds at Al/Ti interface in pure Al antioxidant coatings. *Mater Today Commun*. 2020. <https://doi.org/10.1016/j.mtcomm.2020.101192>.
28. Stoloff SN, Sikka V. *Physical metallurgy and processing of intermetallic compounds*. New York: Springer; 2012.
29. Petrzak P, Mania I, Paul H, Maj Ł, Gałka A. The kinetic of Al₃Ti phase growth in explosively welded multilayered Al/Ti clads during annealing under load conditions. *Mater: Arch. Metall*; 2019. p. 1549.
30. Assari AM, Eghbali B. Microstructure and kinetics of intermetallic phase formation during solid state diffusion bonding in bimetal Ti/Al. *Phys Met Metallogr*. 2019. <https://doi.org/10.1134/S0031918X19030025>.
31. Fronczek DM, Chulist R, Lityńska-Dobrzyńska L, Szulc Z, Zieba P, Wojewoda-Budka J. Microstructure changes and phase growth occurring at the interface of the Al/Ti explosively welded and annealed joints. *J Mater Eng Perform*. 2016. <https://doi.org/10.1007/s11665-016-1978-7>.
32. Xu L, Cui YY, Hao YL, Yang R. Growth of intermetallic layer in multi-laminated Ti/Al diffusion couples. *Mater Sci Eng A*. 2006. <https://doi.org/10.1016/j.msea.2006.07.077>.
33. Loo FJJ, Rieck GD. Diffusion in the titanium-aluminium system-I Interdiff Solid Al Ti Or Ti-Al Alloys. *Acta Metall*. 1973. [https://doi.org/10.1016/0001-6160\(73\)90220-4](https://doi.org/10.1016/0001-6160(73)90220-4).
34. Fronczek DM, Wierzbicka-Miernik A, Saksł K, Miernik K, Chulist R, Kalita D, Szulc Z, Wojewoda-Budka J. The intermetallics growth at the interface of explosively welded Al₁₀₅₀/Ti gr 2/Al₁₀₅₀ clads in relation to the explosive material. *Arch: Civ. Mech. Eng*; 2018. <https://doi.org/10.1016/j.acme.2018.07.007>.
35. Dybkov VI. *Reaction diffusion and solid state chemical kinetics*. Baech: Trans Tech Publications Ltd; 2010.
36. Foadian F, Soltanieh M, Adeli M, Etmianbakhsh M. A study on the formation of intermetallics during the heat treatment of explosively welded Al-Ti multilayers. *Metall: Mater. Trans. A Phys. Metall. Mater. Sci*; 2014. <https://doi.org/10.1007/s11661-013-2144-6>.
37. Assari AH, Eghbali B. Solid state diffusion bonding characteristics at the interfaces of Ti and Al layers. *J Alloys Compd*. 2019. <https://doi.org/10.1016/j.jallcom.2018.09.253>.
38. Foadian F, Soltanieh M, Adeli M, Etmianbakhsh M. The formation of TiAl₃ during heat treatment in explosively welded Ti-Al multilayers. *Iran J Mater Sci Eng*. 2014;11:12–9.
39. Fronczek DM, Chulist R, Szulc Z, Wojewoda-Budka J. Growth kinetics of TiAl₃ phase in annealed Al/Ti/Al explosively welded clads. *Mater Lett*. 2017. <https://doi.org/10.1016/j.matlet.2017.04.025>.
40. Thiyaneashwaran N, Sivaprasad K, Ravisankar B. Characterization based analysis on TiAl₃ intermetallic phase layer growth phenomenon and kinetics in diffusion bonded Ti/TiAl₃/Al laminates. *Mater Charact*. 2021. <https://doi.org/10.1016/j.matchar.2021.110981>.
41. Hu H, Wu X, Wang R, Jia Z, Li W, Liu Q. Structural stability, mechanical properties and stacking fault energies of TiAl₃ alloyed with Zn, Cu, Ag: first-principles study. *J Alloys Compd*. 2016. <https://doi.org/10.1016/j.jallcom.2016.01.106>.

Publisher's Note Springer Nature remains neutral with regard to jurisdictional claims in published maps and institutional affiliations.